SGN: Sequential Grouping Networks for Instance Segmentation

Shu Liu[†] Jiaya Jia[†,♭] Sanja Fidler[‡] Raquel Urtasun[§,‡]

[†]The Chinese University of Hong Kong [♭]Youtu Lab, Tencent
[§]Uber Advanced Technologies Group [‡]University of Toronto

{sliu, leojia}@cse.cuhk.edu.hk {fidler, urtasun}@cs.toronto.edu

Abstract

In this paper, we propose Sequential Grouping Networks (SGN) to tackle the problem of object instance segmentation. SGNs employ a sequence of neural networks, each solving a sub-grouping problem of increasing semantic complexity in order to gradually compose objects out of pixels. In particular, the first network aims to group pixels along each image row and column by predicting horizontal and vertical object breakpoints. These breakpoints are then used to create line segments. By exploiting two-directional information, the second network groups horizontal and vertical lines into connected components. Finally, the third network groups the connected components into object instances. Our experiments show that our SGN significantly outperforms state-of-the-art approaches in both, the Cityscapes dataset as well as PASCAL VOC.

1. Introduction

The community has achieved remarkable progress for tasks such as object detection [32, 10] and semantic segmentation [27, 6] in recent years. Research along these lines opens the door to challenging life-changing tasks, including autonomous driving and personalized robotics.

Instance segmentation is a task that jointly considers object detection and semantic segmentation, by aiming to predict a pixel-wise mask for each object in an image. The problem is inherently combinatorial, requiring us to group sets of pixels into coherent components. Occlusion and vastly varying number of objects across scenes further increase the complexity of the task. In street scenes, such as those in the Cityscapes dataset [7], current methods merely reach 20% accuracy in terms of average precision, which is still far from satisfactory.

Most of the instance segmentation approaches employ a two-step process by treating the problem as a foreground-background pixel labeling task within the object detection boxes [15, 16, 1, 29, 30]. Instead of labeling pixels, [4] predicts a polygon outlining the object instance using a Recurrent Neural Network (RNN). In [41, 40], large patches are exhaustively extracted from an image and a Convolutional Neural Network (CNN) is trained to predict instance labels inside each patch. A dense Conditional Random Field (CRF) is then used to get consistent labeling of the full image. In [33, 31], an RNN is used to produce one object mask per time step. The latter approaches face difficulties on images of street scenes which contain many objects. More recently, [3] learned a convolutional net to predict the energy of the watershed transform. Its complexity does not depend on the number of objects in the scene.

In this paper, we break the task of object instance segmentation into several sub-tasks that are easier to tackle. We propose a grouping approach that employs a sequence of neural networks to gradually compose objects from simpler constituents. In particular, the first network aims to group pixels along each image row and column by predicting horizontal and vertical object breakpoints. These are then used to create horizontal and vertical line segments. The second neural network groups these line segments into connected components. The last network merges components into coherent object instances, thus solving the problem of object splitting due to occlusion. Due to its sequential nature, we call our approach Sequential Grouping Networks (SGN). We evaluate our method on the challenging Cityscapes dataset. SGN significantly outperforms state-of-the-art, achieving a 5% absolute and 25% relative boost in accuracy. We also improve over state-of-the-art on PASCAL VOC for general object instance segmentation which further showcases the strengths of our proposed approach.

2. Related Work

The pioneering work of instance segmentation [15, 8] aimed at both classifying object proposals as well as labeling an object within each box. In [29, 30], high-quality mask proposals were generated using CNNs. Similarly, MNC [9] designed an end-to-end trainable multi-task network cascade to unify bounding box proposal generation, pixel-wise mask proposal generation and classifica-

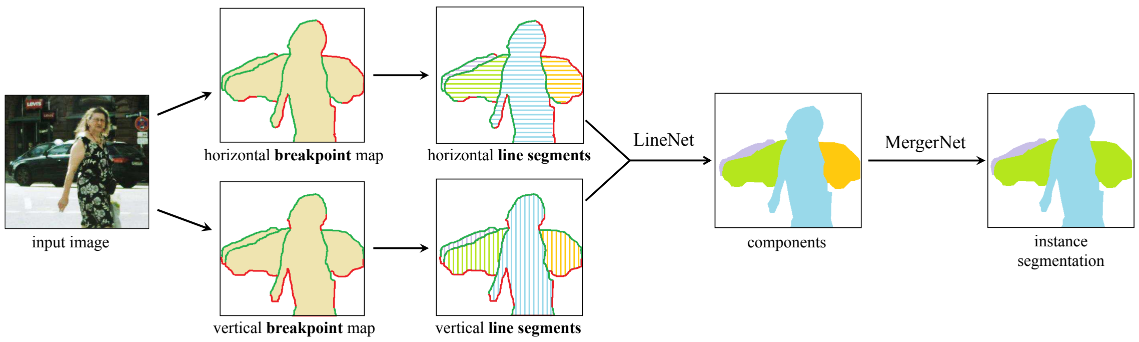
input image
horizontal **breakpoint** map
horizontal **line segments**
vertical **breakpoint** map
vertical **line segments**
LineNet
components
MergerNet
instance segmentation

Figure 1. **Sequential Grouping Networks (SGN):** We first predict breakpoints. LineNet groups them into connected components, which are finally composed by the MergerNet to form our final instances.

tion. SAIS [16] improved MNC by learning to predict distances to instance boundaries, which are then decoded into high-quality masks by a set of convolution operations. A recursive process was proposed in [22] to iteratively refine the predicted pixel-wise masks. Recently, [4] proposed to predict polygons outlining each object instance which has the advantage of efficiently capturing object shape.

MPA [26] modeled objects as composed of generic parts, which are predicted in a sliding window fashion and then aggregated to produce instances. IIS [20] is an iterative approach to refine the instance masks. In [21], the authors utilized a fully convolutional network by learning to combine different relative parts into an instance. Methods of [41, 40] extracted patches from the image and used a CNN to directly infer instance IDs inside each patch. A CRF is then used to derive globally consistent labels of the image.

In [1, 2], a CRF is used to assign each pixel to an object detection box by exploiting semantic segmentation maps. Similarly, PFN [23] utilized semantic segmentation to predict the bounding box each pixel belongs to. Pixels are then grouped into clusters based on the distances to the predicted bounding boxes. In [36], the authors predict the direction to the instance's center for each pixel, and exploits templates to infer the location of instances on the predicted angle map.

Recently, Bai and Urtasun [3] utilized a CNN to learn an energy of the watershed transform. Instances naturally correspond to basins in the energy map. It avoids the combinatorial complexity of instance segmentation. In [18], semantic segmentation and object boundary prediction were exploited to separate instances. Different types of label transformation were investigated in [17]. Pixel association was learned in [28] to differentiate between instances.

Finally, RNN [33, 31] was used to predict an object label at each time step. However, since RNNs typically do not perform well when the number of time steps is large, these methods have difficulties in scaling up to the challenging multi-object street scenes.

Here, we propose a new type of approach to instance segmentation by exploiting several neural networks in a sequential manner, each solving a sub-grouping problem.

3. Sequential Grouping Networks

In this section, we present our approach to object instance segmentation. Following [3, 18], we utilize semantic segmentation to identify foreground pixels, and restrict our reasoning to them. We regard instances as composed of breakpoints that form line segments, which are then combined to generate full instances. Fig. 1 illustrates our model. We first introduce the network to identify breakpoints, and show how to use them to group pixels into lines in Subsec. 3.2. In Subsec. 3.3, we propose a network that groups lines into components, and finally the network to group components into instances is introduced in Subsec. 3.4.

3.1. Predicting Breakpoints

Our most basic primitives are defined as the pixel locations of *breakpoints*, which, for a given direction, represent the beginning or end of each object instance. Note that we reason about the breakpoints in both the horizontal and vertical direction. For the horizontal direction, computing the starting points amounts to scanning the image from left to right, one row at a time, recording the change points where a new instance appears. For the vertical direction, the same process is conducted from top to bottom. As a consequence, the boundary between instances is considered as a starting point. The termination points are then the pixels where an instance has a boundary with the background. Note that this is different from predicting standard boundaries as it additionally encodes the direction where the interior of the instance is.

We empirically found that introducing two additional labels encoding the instance interior as well as the background is helpful to make the end-point prediction sharper. Each pixel in an image is thus labeled with 4 labels encoding either background, interior, starting point or a termination point. We refer the reader to Fig. 1 for an example.

Network Structure We exploit a CNN to perform this pixel-wise labeling task. The network takes the original image as input and predicts two label maps, one per direction as shown in Fig. 2(a). Our network is based on Deeplab-

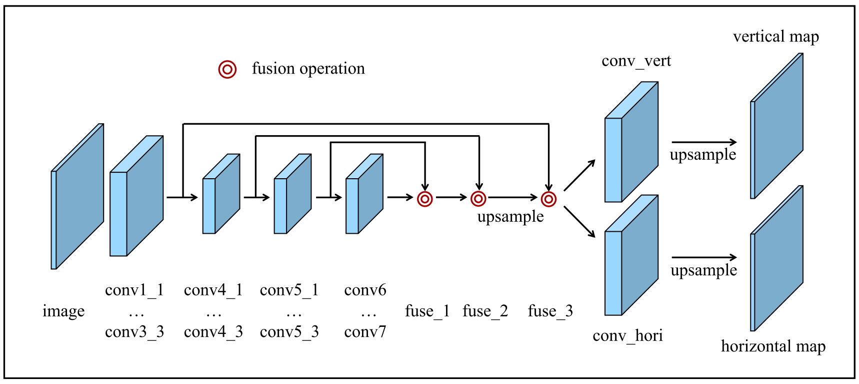

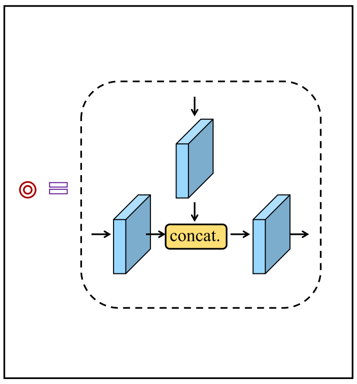

Figure 2. Illustration of **(a)** network structure for predicting breakpoints, and **(b)** the fusion operation.

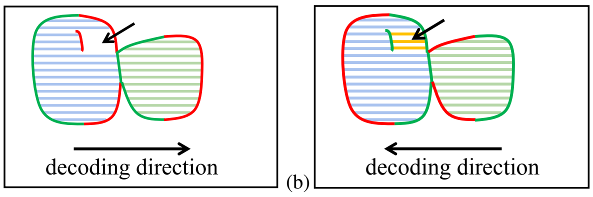

Figure 3. **Line decoding process**. Green and red points are starting and termination ones. Scanning from left to right, there is no more line segment in the area pointed by the black arrow in **(a)** due to erroneous point detection. The reversal scanning in **(b)** gets new line hypothesis in this area, shown by orange line segments.

LargeFOV [5]. We use a modified VGG16 [35], and make it fully convolutional as in FCN [27]. To preserve precise localization information, we remove *pool4* and *pool5* layers. To enlarge the receptive field, we make use of dilated convolutions [39, 6] in the *conv5* and *conv6* layers.

Similar to the methods in [30, 24, 12], we augment the network by connecting lower layers to higher ones in order to capture fine details. In particular, we fuse information from *conv5_3, conv4_3* and *conv3_3* layers, as shown in Fig. 2 (b). To be more specific, we first independently filter the input feature maps through 128 filters of size 3×3, which are then concatenated. We then utilize another set of 128 filters of size 3×3 to decrease the feature dimension. After fusion with *conv3_3*, the feature map is downscaled by a factor of 4. Predictions for breakpoint maps are then made by two independent branches on top of it.

Learning Predicting breakpoints is hard since they are very sparse, making the distribution of labels unbalanced and dominated by the background and interior pixels. To mitigate this effect, similar to HED [38], we re-weight the cross-entropy loss based on inverse of the frequency of each class in the mini-batch.

3.2. Grouping Breakpoints into Line Segments

Since the convolutional net outputs breakpoints that span over multiple consecutive pixels, we use a morphological operator to create boundaries with one pixel width. We further augment the set of breakpoints with the boundaries in the semantic segmentation prediction map to ensure we do not miss any boundary. We then design an algorithm that reverses the process of generating breakpoints from instance segmentation in order to create line segments. To create horizontal lines, we slide from left to right along each row, and start a new line when we hit a starting point. Lines are terminated when we hit an end point or a new starting point. The latter arises at the boundary of two different instances. Fig. 3 (a) illustrates this process. To create vertical lines, we perform similar operations but slide from top to bottom.

This simple process inevitably introduces errors if there are false termination points inside instances. As shown in Fig. 3 (a), the area pointed by the black arrow is caused by false termination points. To handle this issue, we augment the generated line segments by decoding in the reverse direction (right to left for horizontal lines and bottom to top for vertical ones) as illustrated in Fig. 3 (b). Towards this goal, we identify the starting points lying between instances by counting the consecutive number of starting points. We then switch starting and termination points for all points that are not double starting points and decode in the reverse order. As shown in Fig. 3 (b), this simple process gives us the additional lines (orange) necessary to complete the instance.

3.3. Grouping Lines into Connected Components

The next step is to aggregate lines to create instances that form a single connected component. We utilize the horizontal lines as our elements and recursively decide whether to merge a line into an existing component. Note that this is an efficient process since there are much fewer lines compared to raw pixels. On average, the number of operations that need to be made is 4802 per image on Cityscapes and 1014 on PASCAL VOC. Our merging process is performed by a memory-less recurrent network, which we call *LineNet*. *LineNet* scans the image from top to bottom and sequentially decides whether to merge the new line into one of the existing neighboring instances (i.e., instances that touch the line in at least one pixel). An example is shown in Fig. 4 (a) where O_k is an instance and s_i is a line segment.

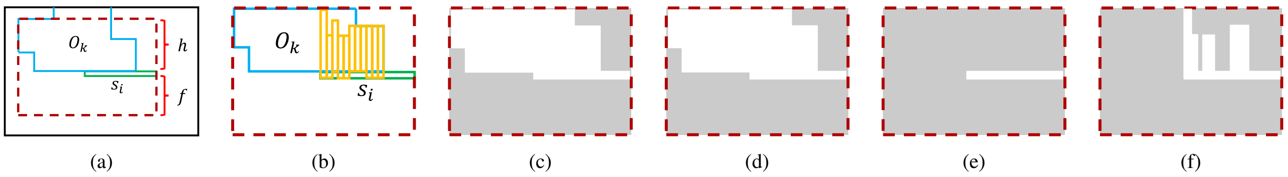

Figure 4. **(a)** Context area is highlighted in the dashed red bounding box. **(b)** Orange vertical rectangles represent vertical line segments. **(c)** First channel. **(d)** Second channel where O_k and s_i have the same semantic class. **(e)** The situation when O_k and s_i are not in the same class. **(f)** Third channel.

Network Structure Let s_i be the line segment we consider and O_k is an instance in Fig. 4 (a). LineNet uses as context a small number of rows h on top of s_i encoding the history of already merged instances, as well as a small set of rows f below s_i encoding the future possible merges. We restrict the horizontal context to be the minimum interval containing the instance candidate O_k and the line s_i. This is shown as the dashed red area in Fig. 4 (a). We also pad zeros to make the window horizontally centered at s_i and resize the window horizontally to have a fixed size.

The input to LineNet contains 9 channels. The first is a boolean map with ones in the pixels belonging to s_i or O_k. The second channel contains ones for pixels in O_k that are labeled in the same semantic class as the majority of the pixels in line s_i. The third channel is a boolean map showing pixels in O_k that share the same vertical line segment with s_i. The first three channels are illustrated in Fig. 4 (c)-(f). Additionally, we append 6 channels containing the interior and breakpoint probability maps in the vertical and horizontal directions. LineNet is a very small net, consisting of two shared fully-connected layers and class-specific classifiers with the sigmoid function. The output for each semantic class is the probability of merging the line with the candidate instance.

Learning We use standard cross-entropy loss to train LineNet, where a line should be merged with an existing instance if the majority of pixels in the line and instance belong to the same ground-truth instance.

3.4. Merging Fragmented Instances

Note that many instances are composed of more than one connected component. This is the case for example of a car that is occluded by a pole, as shown in Fig. 5 (a). This issue is common in urban scenes. On average 3.5 instances per image are fragmented in Cityscapes. In PASCAL, this number is much smaller with only 0.3 instance per image.

In order to deal with fragmented instances, we design a MergerNet that groups these components to form the final set of object instances. Note that most instance segmentation algorithms cannot tackle the fragmentation problem [3, 26, 18, 41, 40]. Our MergerNet can thus also be used to enhance these approaches. In particular, as merging candidates for each segment we choose all segments that are closer than a fixed threshold. We use 100 pixels in practice.

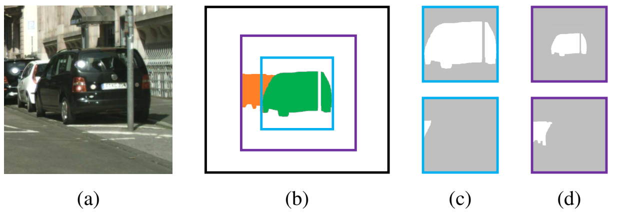

Figure 5. **(a)** A car that is occluded by a pole resulting in fragmented parts. **(b)** Bounding boxes containing the current pair, *i.e.*, two green segments. **(c)** First two input channels. **(d)** Sixth and seventh input channels to the MergerNet.

We then order these segments by size, and utilize a memory-less recurrent net to further decide whether to merge or not. If a merge occurs, we recompute the set of neighbors and repeat this process.

Network Architecture Our *MergerNet* takes as input 10 channels. To generate the first 5 channels, we fit a tight square bounding box containing candidate regions (blue box in Fig. 5 (b)) and generate the representation within this box. The first channel is a boolean map with ones for pixels belonging to either instance. The second channel is a boolean map with ones indicating other segments lying in the box. This provides information about other possible merges. Fig. 5 (c) shows the first two channels. The next three channels are simply the image RGB values in this bounding box. We resize all channels to a fixed size of 128×128. The remaining 5 channels are generated in a similar way except that they are from a bounding box doubled the size (purple box in Fig. 5 (b)). The sixth and seventh channels are illustrated in Fig. 5 (d). The network is small, consisting of 3 convolution layers, one shared fully-connected layer and class-specific classifiers with sigmoid function to produce the final merge probability.

Learning We generate training samples for MergerNet by running inference on the training images and use the ground-truth instances to infer whether the different components should be merged or not. In particular, we merge them if the majority of pixels are part of the same GT instance. We use standard cross-entropy as the loss function for each class. The result of this merging process is our final instance segmentation. We define the semantic label of each instance as the class that the majority of pixels are labeled.

Method	person	rider	car	truck	bus	train	mcycle	bicycle
Uhrig *et al.* [36]	12.5	11.7	22.5	3.3	5.9	3.2	6.9	5.1
RecAttend [31]	9.2	3.1	27.5	8.0	12.1	7.9	4.8	3.3
Levinkov *et al.* [19]	6.5	9.3	23.0	6.7	10.9	10.3	6.8	4.6
InstanceCut [18]	10.0	8.0	23.7	14.0	19.5	15.2	9.3	4.7
SAIS [16]	14.6	12.9	35.7	16.0	23.2	19.0	10.3	7.8
DWT [3]	15.5	14.1	31.5	22.5	27.0	22.9	13.9	8.0
DIN [1]	16.5	16.7	25.7	20.6	30.0	23.4	17.1	10.1
Our SGN	**21.8**	**20.1**	**39.4**	**24.8**	**33.2**	**30.8**	**17.7**	**12.4**

Method	**AP**	AP 50%	AP 100m	AP 50m
Uhrig *et al.* [36]	8.9	21.1	15.3	16.7
RecAttend [31]	9.5	18.9	16.8	20.9
Levinkov *et al.* [19]	9.8	23.2	16.8	20.3
InstanceCut [18]	13.0	27.9	22.1	26.1
SAIS [16]	17.4	36.7	29.3	34.0
DWT [3]	19.4	35.3	31.4	36.8
DIN [1]	20.0	38.8	32.6	37.6
Our SGN	**25.0**	**44.9**	**38.9**	**44.5**

Table 1. AP results on Cityscapes *test*. The entries with the best performance are bold-faced.

Method	person	rider	car	truck	bus	train	motorcycle	bicycle	AP	AP 50%
DWT-non-ranking [3]	15.5	13.8	33.1	23.6	39.9	17.4	11.9	8.8	20.5	-
DWT-ranking [3]	15.5	13.8	33.1	27.1	45.2	14.5	11.9	8.8	21.2	-
SAIS [16]	-	-	-	-	-	-	-	-	-	32.4
Our SGN	**21.3**	**19.5**	**41.2**	**33.4**	**49.9**	**40.7**	**14.7**	**13.0**	**29.2**	**49.4**

Table 2. AP results on Cityscapes *val*. The entries with the best performance are bold-faced.

4. Experimental Evaluation

We evaluate our method on the challenging dataset Cityscapes [7] as well as PASCAL VOC 2012 [11]. We focus our experiments on Cityscapes as it is much more challenging. On average, it contains 17 object instances per image vs 2.4 in PASCAL.

Dataset The Cityscapes dataset [7] contains imagery of complex urban scenes with high pixel resolution of $1,024 \times 2,048$. There are $5,000$ images with high-quality annotations that are split into subsets of $2,975$ *train*, 500 *val* and $1,525$ *test* images, respectively. We use images in the *train* subset with fine labels to train our networks. For the instance segmentation task, there are 8 classes, including different categories of people and vehicles. Motion blur, occlusion, extreme scale variance and imbalanced class distribution make this dataset extremely challenging.

Metrics The metric used by Cityscapes is Average Precision (AP). It is computed at different thresholds from 0.5 to 0.95 with step-size of 0.05 followed by averaging. We report AP at 0.5 IoU threshold and AP within a certain distance. As pointed in [3, 1], AP favors detection-based methods. Thus we also report the Mean Weighted Coverage (MWCov) [31, 37], which is the average IoU of prediction matched with ground-truth instances weighted by the size of the ground-truth instances.

Implementation Details For our breakpoint prediction network, we initialize *conv1* to *conv5* layers from VGG16 [35] pre-trained on Imagenet [34]. We use random initialization for other layers. The learning rates to train the breakpoint prediction network, LineNet and the MergerNet are set to 10^{-5}, 10^{-2} and 10^{-3}, respectively. We use SGD with momentum for training. Following the method of [5], we use the "poly" policy to adjust the learning rate. We train the breakpoint prediction network for 40k iterations, while LineNet and MergerNet are trained using 20k iterations. To alleviate the imbalance of class distribution for LineNet and MergerNet, we sample training examples in mini-batches by keeping equal numbers of positives and negatives. Following [3], we remove small instances and use semantic scores from semantic segmentation to rank predictions for $\{$*train, bus, car, truck*$\}$. For other classes, scores are set to 1. By default, we use semantic segmentation prediction from PSP [42] on Cityscapes and LRR [13] on PASCAL VOC. We also conduct an ablation study of how the quality of semantic segmentation influences our results.

Comparison to State-of-the-art As shown in Table 1, our approach significantly outperforms other methods on all classes. We achieve an improvement of 5% absolute and 25% in relative performance compared to state-of-the-art reported on the Cityscapes website, captured at the moment of our submission. We also report results on the validation set in Table 2, where the improvement is even larger.

Influence of Semantic Segmentation We investigate the influence of semantic segmentation in our instance prediction approach. We compare the performance of our approach when using LRR [13], which is based on VGG-16, with PSP [42], which is based on Resnet-101. As shown in Table 3, we achieve reasonable results using LRR, however, much better results are obtained when exploiting PSP. Results improve significantly in both cases when using the MergerNet. Note that LineNet and MergerNet are not fine-tuned for LRR prediction.

Influence of Size As shown in Fig. 7, as expected, small instances are more difficult to detect than the larger ones.

Influence of LineNet Parameters The contextual information passed to LineNet is controlled by the number of history rows h, as well as the number of rows f encoding the future information. As shown in Table 4, LineNet is not

LRR [13]	PSP [42]	MergerNet	AP	AP 50%	MWCov
✓			20.0	37.8	64.3
✓		✓	21.7	40.9	66.4
	✓		25.2	43.8	70.6
	✓	✓	**29.2**	**49.4**	**74.1**

Table 3. Cityscapes *val* with different semantic segm. methods.

Metric	h1f1	h1f3	h1f5	h3f1	h3f3	h3f5	h5f1	h5f3	h5f5
AP	**25.3**	25.2	25.2	24.8	24.9	24.9	24.9	25.2	25.0
AP 50%	44.0	**44.1**	43.8	43.2	43.6	43.3	43.3	43.7	43.5
MWCov	71.4	71.3	**71.6**	70.9	71.5	71.3	71.1	**71.6**	71.4

Table 4. Cityscapes *val* results in terms of AP, AP 50%, MWCov.

sensitive to the context parameters while local information is sufficient. In the following experiments, we select the entry “h1f5” by considering both AP and MWCov.

Heuristic Methods vs LineNet We compare LineNet to two heuristic baseline methods. The first takes the union of vertical and horizontal breakpoints and class boundaries from PSP. We thin them into one pixel width to get the instance boundary map. In the foreground area defined via the PSP semantic segmentation map, we set the instance boundary as 0 and then take connected components as inferred instances. Post-processing steps, such as removing small objects and assigning scores, are exactly the same as in our approach. We name this method “con-com”.

Our second baseline is called “heuristic”. Instead of using LineNet, we simply calculate a relationship between two neighboring line segments (current line segment and neighboring line segment in previous row) to make a decision. The value we compute includes the IoU value, ratio of the overlaps with the other line segment and ratio of vertical line segments connecting them in the overlapping area. If each value and their summation are higher than the chosen thresholds, we merge the two line segments. This strategy simply makes decisions based on the current line segment pair – no training is needed.

As shown in Table 6, on average, the heuristic strategy outperforms the simple connected component method in terms of all metrics. This clearly shows the benefit of using line segments. LineNet outperforms both heuristic methods, demonstrating the advantage of incorporating a network to perform grouping. The connected component method performs quite well on classes such as *car* and *bus*, but performs worse on *person* and *motorcycle*. This suggests that boundaries are more beneficial to instances with compact shape than to those with complex silhouettes. Our approach, however, works generally well on both, complex and compact shapes, and further enables networks to correct errors that exist in breakpoint maps.

Influence of MergerNet Parameters A parameter of the MergerNet is the max distance between foreground regions

Method	AP^r					AP^r_{avg}
	0.5	0.6	0.7	0.8	0.9	
PFN [23]	58.7	51.3	42.5	31.2	15.7	39.9
Arnab *et al.* [2]	58.3	52.4	45.4	34.9	20.1	42.2
MPA 3-scale [26]	**62.1**	**56.6**	47.4	36.1	18.5	44.1
DIN [1]	61.7	55.5	48.6	39.5	25.1	46.1
Our SGN	61.4	55.9	**49.9**	**42.1**	**26.9**	**47.2**

Table 5. AP^r on PASCAL *val*.

in a candidate pair. To set the value, we first predict instances with LineNet on the *train* subset and compute statistics. We show recall of pairs that need to be merged vs distance in Fig. 8(a) and the number of pairs with distance smaller than a threshold vs distance in Fig. 8(b). We plot the performance with respect to different maximum distances used to merge in Fig. 8(c) and (d). Distance 0 means that the MergerNet is not utilized. The MergerNet with different parameters consistently improves performance. The results show that the MergerNet with 150 pixels as the maximum distance performs slightly worse than MergerNet with 50 and 100 pixels. We hypothesize that with larger distances, more false positives confuse MergerNet during inference.

Visual Results We show qualitative results of all intermediate steps in our approach on Cityscapes *val* in Fig. 6. Our method produces high-quality breakpoints, instance interior, line segments and final results, for objects of different scales, classes and occlusion levels. The MergerNet works quite well as shown in Fig. 6 as well as on the *train* object in Fig. 9(b). Note that predictions with IoU higher than 0.5 are assigned colors of their corresponding ground-truth labels.

Failure Modes Our method may fail if errors exist in the semantic segmentation maps. As shown in Fig. 9(b), a small part of the *train* is miss-classified by PSP. So the *train* is broken into two parts. Our method may also miss extremely small instances, such as some *people* in Fig. 9(e) and (f). Further, when several complex instances are close to each other, we may end up grouping them as shown in Fig. 9(g) and (h). The MergerNet sometimes also aggregates different instances such as the two light green *cars* in Fig. 9(a).

Results on PASCAL VOC We also conduct experiments on PASCAL VOC 2012 [11], which contains 20 classes. As is common practice, for training images, we additionally use annotations from the SBD dataset [14], resulting in $10,582$ images with instance annotation. For the *val* subset, we used $1,449$ images from VOC 2012 *val* set. There is no overlap between training and validation images. Following common practice, we compare with state-of-the-art on the *val* subset since there is no held-out test set. Note that the LRR model we use is pre-trained on MS COCO [25], which is also used by DIN [1] for pre-training.

We use AP^r [15] as the evaluation metric, representing the region AP at a specific IoU threshold. Following [25, 7],

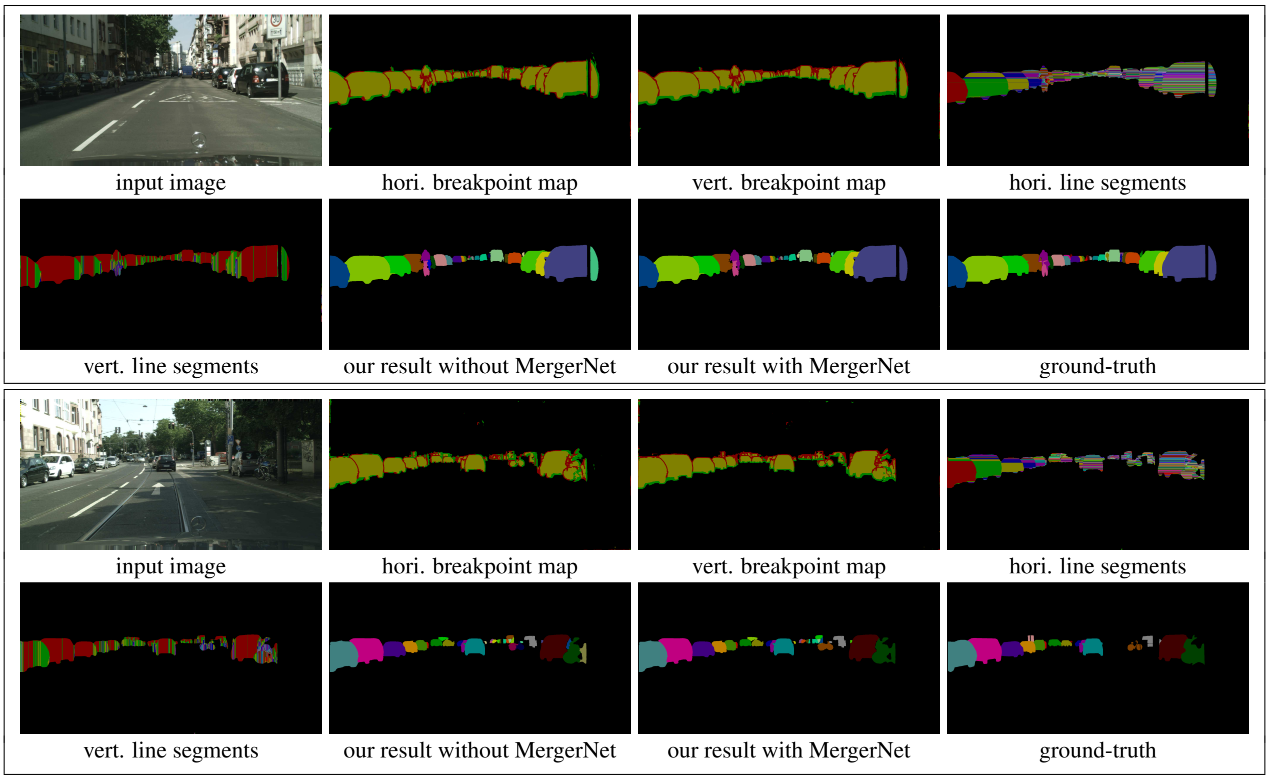

Figure 6. Qualitative results of all intermediate results and final prediction.

Method	person	rider	car	truck	bus	train	motorcycle	bicycle	Average
con-com	16.6 / 70.8	9.1 / 57.2	**40.0 / 89.6**	29.8 / **84.5**	**46.6** / 88.8	21.1 / 68.5	7.4 / 48.9	6.1 / 49.1	22.1 / 69.7
heuristic	**20.4 / 71.7**	16.1 / 62.0	36.6 / 87.3	29.0 / 80.8	38.5 / **89.3**	19.4 / 68.7	10.1 / 54.2	8.4 / **50.9**	23.6 / 70.6
Linenet	20.2 / **71.7**	**17.8 / 62.9**	38.5 / 88.2	**32.0** / 83.9	46.4 / 88.6	**23.3 / 69.5**	**14.1 / 59.4**	**9.4** / 48.4	**25.2 / 71.6**

Table 6. Results on Cityscapes *val* in terms of AP / MWCov.

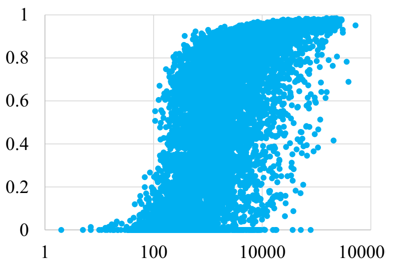

Figure 7. IoU as a function of ground-truth sizes.

we average AP^r at IoU threshold ranging from 0.5 to 0.9 with step-size 0.1 (instead of 0.1 to 0.9). We believe that AP^r at higher IoU thresholds are more informative.

As shown in Table 5 our method outperforms DIN [1] by 1.1 points in terms of AP$^r_{\text{avg}}$. We also achieve better performance for IoU higher than 0.6. This result demonstrates the quality of masks generated by our method. Our method takes about 2.2s with LineNet "h1f5" and 1.6s with LineNet "h1f1" per image using one Titan X graphics card and an Intel Core i7 3.50GHZ CPU using a single thread on PASCAL VOC. This includes the CPU time.

5. Conclusion

We proposed Sequential Grouping Networks (SGN) for object instance segmentation. Our approach employs a sequence of simple networks, each solving a more complex grouping problem. Object breakpoints are composed to create line segments, which are then grouped into connected components. Finally, the connected components are grouped into full objects. Our experiments showed that our approach significantly outperforms existing approaches on the challenging Cityscapes dataset and works well on PASCAL VOC. In our future work, we plan to make our framework end-to-end trainable.

6. Acknowledgments

This work is in part supported by NSERC, CFI, ORF, ERA, CRC as well as Research Grants Council of the Hong Kong SAR (project No. 413113). We also acknowledge GPU donations from NVIDIA.

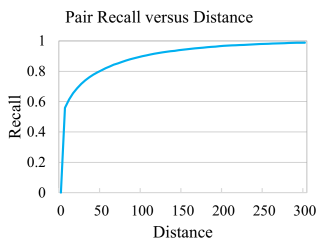

(a)

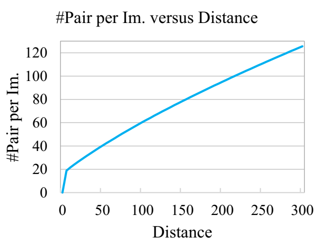

(b)

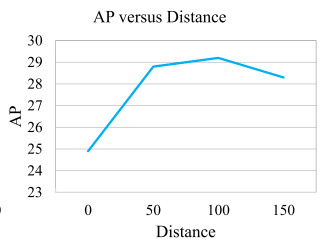

(c)

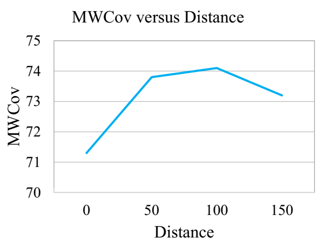

(d)

Figure 8. **(a)** Recall of merge pairs as a function of max distance. **(b)** Number of pairs with distance of foreground regions smaller than a distance. **(c)** AP with respect to different maximum distances. **(d)** MWCov with respect to different maximum distances.

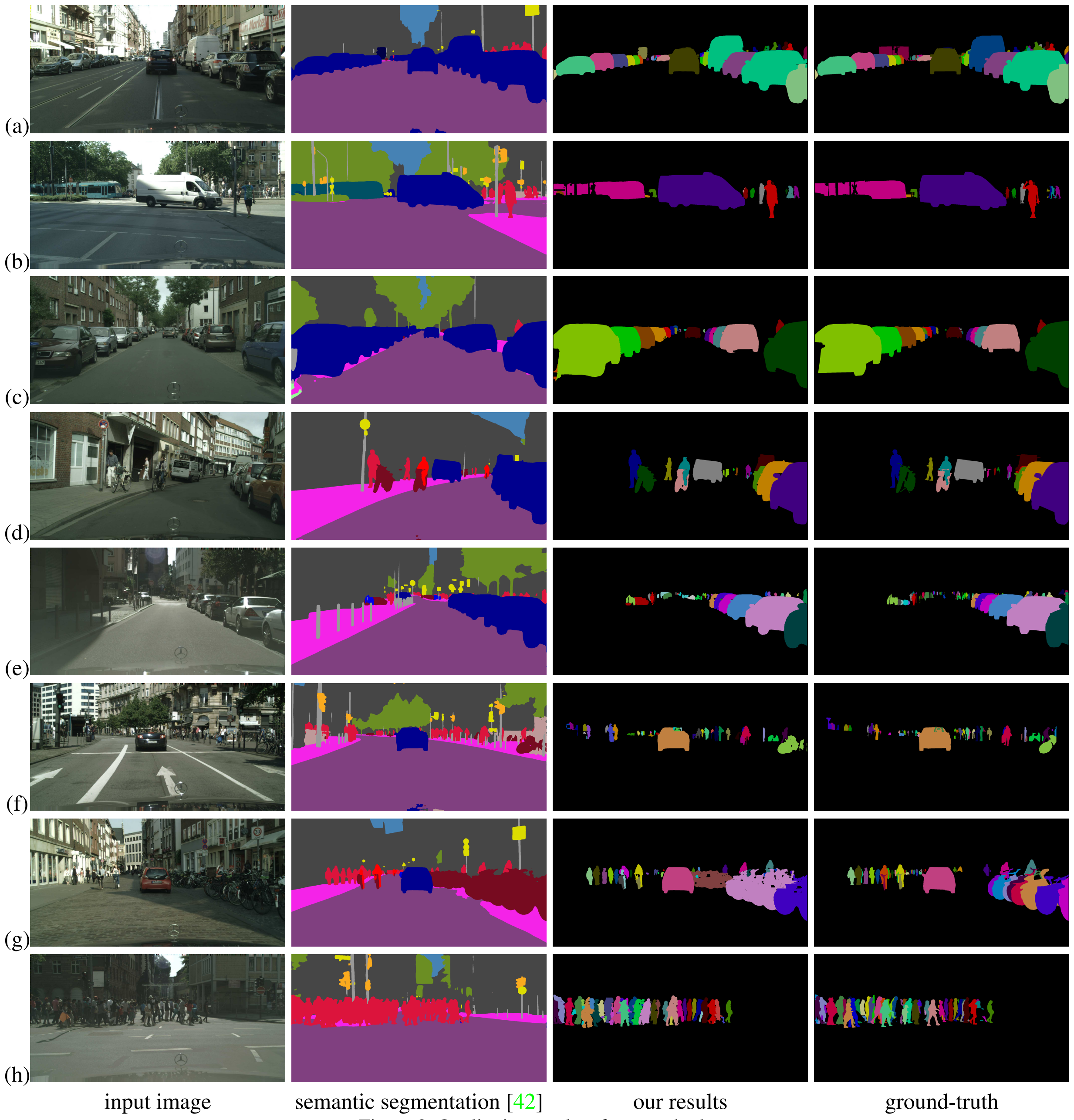

Figure 9. Qualitative results of our method.

References

[1] A. Arnab and P. H. Torr. Pixelwise instance segmentation with a dynamically instantiated network. In *CVPR*, 2017. 1, 2, 5, 6, 7

[2] A. Arnab and P. H. S. Torr. Bottom-up instance segmentation using deep higher-order crfs. *CoRR*, 2016. 2, 6

[3] M. Bai and R. Urtasun. Deep watershed transform for instance segmentation. *CoRR*, 2016. 1, 2, 4, 5

[4] L. Castrejon, K. Kundu, R. Urtasun, and S. Fidler. Annotating object instances with a polygon-rnn. In *CVPR*, 2017. 1, 2

[5] L. Chen, G. Papandreou, I. Kokkinos, K. Murphy, and A. L. Yuille. Deeplab: Semantic image segmentation with deep convolutional nets, atrous convolution, and fully connected crfs. *CoRR*, 2016. 3, 5

[6] L.-C. Chen, G. Papandreou, I. Kokkinos, K. Murphy, and A. L. Yuille. Semantic image segmentation with deep convolutional nets and fully connected crfs. In *ICLR*, 2015. 1, 3

[7] M. Cordts, M. Omran, S. Ramos, T. Rehfeld, M. Enzweiler, R. Benenson, U. Franke, S. Roth, and B. Schiele. The cityscapes dataset for semantic urban scene understanding. In *CVPR*, 2016. 1, 5, 6

[8] J. Dai, K. He, and J. Sun. Convolutional feature masking for joint object and stuff segmentation. In *CVPR*, 2015. 1

[9] J. Dai, K. He, and J. Sun. Instance-aware semantic segmentation via multi-task network cascades. *CVPR*, 2016. 1

[10] J. Dai, Y. Li, K. He, and J. Sun. R-FCN: object detection via region-based fully convolutional networks. *CoRR*, 2016. 1

[11] M. Everingham, L. Van Gool, C. K. Williams, J. Winn, and A. Zisserman. The pascal visual object classes (voc) challenge. *IJCV*, 2010. 5, 6

[12] C. Fu, W. Liu, A. Ranga, A. Tyagi, and A. C. Berg. DSSD : Deconvolutional single shot detector. *CoRR*, 2017. 3

[13] G. Ghiasi and C. C. Fowlkes. Laplacian reconstruction and refinement for semantic segmentation. *CoRR*, 2016. 5, 6

[14] B. Hariharan, P. Arbelaez, L. Bourdev, S. Maji, and J. Malik. Semantic contours from inverse detectors. In *ICCV*, 2011. 6

[15] B. Hariharan, P. Arbeláez, R. Girshick, and J. Malik. Simultaneous detection and segmentation. In *ECCV*. 2014. 1, 6

[16] Z. Hayder, X. He, and M. Salzmann. Shape-aware instance segmentation. *CoRR*, 2016. 1, 2, 5

[17] L. Jin, Z. Chen, and Z. Tu. Object detection free instance segmentation with labeling transformations. *CoRR*, 2016. 2

[18] A. Kirillov, E. Levinkov, B. Andres, B. Savchynskyy, and C. Rother. Instancecut: from edges to instances with multicut. *CoRR*, 2016. 2, 4, 5

[19] E. Levinkov, S. Tang, E. Insafutdinov, and B. Andres. Joint graph decomposition and node labeling by local search. *CoRR*, 2016. 5

[20] K. Li, B. Hariharan, and J. Malik. Iterative instance segmentation. *CVPR*, 2016. 2

[21] Y. Li, H. Qi, J. Dai, X. Ji, and Y. Wei. Fully convolutional instance-aware semantic segmentation. *CoRR*, 2016. 2

[22] X. Liang, Y. Wei, X. Shen, Z. Jie, J. Feng, L. Lin, and S. Yan. Reversible recursive instance-level object segmentation. *arXiv*, 2015. 2

[23] X. Liang, Y. Wei, X. Shen, J. Yang, L. Lin, and S. Yan. Proposal-free network for instance-level object segmentation. *arXiv*, 2015. 2, 6

[24] T. Lin, P. Dollár, R. B. Girshick, K. He, B. Hariharan, and S. J. Belongie. Feature pyramid networks for object detection. *CoRR*, 2016. 3

[25] T.-Y. Lin, M. Maire, S. Belongie, J. Hays, P. Perona, D. Ramanan, P. Dollár, and C. L. Zitnick. Microsoft coco: Common objects in context. In *ECCV*. 2014. 6

[26] S. Liu, X. Qi, J. Shi, H. Zhang, and J. Jia. Multi-scale patch aggregation (mpa) for simultaneous detection and segmentation. *CVPR*, 2016. 2, 4, 6

[27] J. Long, E. Shelhamer, and T. Darrell. Fully convolutional networks for semantic segmentation. In *CVPR*, 2015. 1, 3

[28] A. Newell and J. Deng. Associative embedding: End-to-end learning for joint detection and grouping. *CoRR*, 2016. 2

[29] P. H. O. Pinheiro, R. Collobert, and P. Dollár. Learning to segment object candidates. In *NIPS*, 2015. 1

[30] P. H. O. Pinheiro, T. Lin, R. Collobert, and P. Dollár. Learning to refine object segments. In *ECCV*, 2016. 1, 3

[31] M. Ren and R. S. Zemel. End-to-end instance segmentation and counting with recurrent attention. *CoRR*, 2016. 1, 2, 5

[32] S. Ren, K. He, R. Girshick, and J. Sun. Faster r-cnn: Towards real-time object detection with region proposal networks. In *NIPS*, 2015. 1

[33] B. Romera-Paredes and P. H. S. Torr. Recurrent instance segmentation. *CoRR*, 2015. 1, 2

[34] O. Russakovsky, J. Deng, H. Su, J. Krause, S. Satheesh, S. Ma, Z. Huang, A. Karpathy, A. Khosla, M. S. Bernstein, A. C. Berg, and F. Li. Imagenet large scale visual recognition challenge. *International Journal of Computer Vision*, 2015. 5

[35] K. Simonyan and A. Zisserman. Very deep convolutional networks for large-scale image recognition. *ICLR*, 2014. 3, 5

[36] J. Uhrig, M. Cordts, U. Franke, and T. Brox. Pixel-level encoding and depth layering for instance-level semantic labeling. *CoRR*, 2016. 2, 5

[37] S. Wang, M. Bai, G. Máttyus, H. Chu, W. Luo, B. Yang, J. Liang, J. Cheverie, S. Fidler, and R. Urtasun. Torontocity: Seeing the world with a million eyes. *CoRR*, 2016. 5

[38] S. Xie and Z. Tu. Holistically-nested edge detection. In *ICCV*, 2015. 3

[39] F. Yu and V. Koltun. Multi-scale context aggregation by dilated convolutions. *CoRR*, 2015. 3

[40] Z. Zhang, S. Fidler, and R. Urtasun. Instance-level segmentation for autonomous driving with deep densely connected mrfs. In *CVPR*, 2016. 1, 2, 4

[41] Z. Zhang, A. G. Schwing, S. Fidler, and R. Urtasun. Monocular object instance segmentation and depth ordering with cnns. *CoRR*, 2015. 1, 2, 4

[42] H. Zhao, J. Shi, X. Qi, X. Wang, and J. Jia. Pyramid scene parsing network. *CoRR*, 2016. 5, 6, 8